THE JOURNAL OF PHYSICAL CHEMISTRY C

Article

pubs.acs.org/JPCC

Hydrogen Dissociative Adsorption on Lanthana: Polaron Formation and the Role of Acid−Base Interactions

Steeve Chrétien and Horia Metiu*

Department of Chemistry and Biochemistry, University of California, Santa Barbara, California 93106-9510, United States

Supporting Information

ABSTRACT: Previous work has proposed that two molecules that coadsorb on an irreducible oxide surface tend to choose their binding sites so that one is a Lewis acid and the other is a Lewis base. Here we examine whether this rule works in the case of the adsorption of two hydrogen atoms on lanthana. We find that when one hydrogen atom is adsorbed, it will bind to an oxygen atom and form a polaron by donating electron charge to a group of La atoms. When two atoms are adsorbed, one forms a hydroxyl and the other forms a hydride at the polaron site created by the adsorption of the first atom. Polaron formation in irreducible oxides is rather unusual, and so is the formation of a hydride. While the former is probably limited to lanthana, the latter is likely to be a general feature for all irreducible oxides if an electron donor is present on the surface.

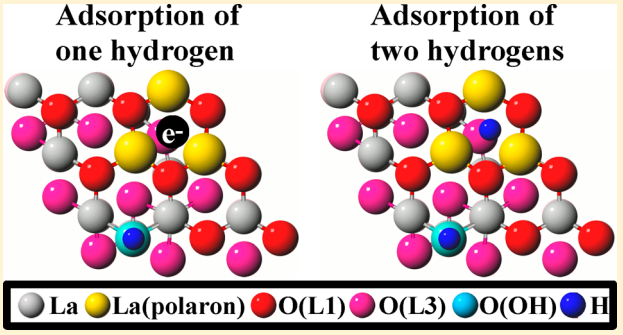

1. INTRODUCTION

Quantum mechanical studies of the coadsorption of two species, A and B, on an oxide surface require many calculations to determine the binding energies on all possible surface sites. Any rule that reduces a priori the number of combinations to be tried would be helpful. One might reasonably expect that when they are coadsorbed on an oxide surface, A and B will bind to the surface sites they prefer when they bind alone. For example, if B binds to an oxygen atom when it is alone, one would think that it will also bind to oxygen when A is already adsorbed on the surface. It would also be reasonable to expect that the energy of coadsorbed A and B is roughly equal to the sum of the energies of binding each species alone. However, several calculations,[1−12] which examined a variety of surfaces and of coadsorbed compounds, found examples in which neither of these expectations is correct: the presence of A on the surface might have a profound influence on the site to which B will bind and on its binding energy. This behavior is consistent with rules[6,8,11] that state that the presence of a Lewis base (an electron donor) on an oxide surface will increase substantially the binding energy of a Lewis acid (an electron acceptor). Examples of Lewis bases are higher valence dopants, an oxygen vacancy, a hydroxyl, CH_3, NH_3, and an alkali-metal atom. Examples of Lewis acids are lower valence dopants, O_2, Br_2, I_2, and Cl_2. Moreover, if at all possible, when A and B are coadsorbed, they will choose their binding sites so that one of them is a Lewis acid and the other is a Lewis base. For example, if HBr is adsorbed dissociatively on an oxide surface, H will bind to the oxygen (to form a hydroxyl in which H is positively charged) and Br will bind to the cation to form Br^-, even though when it binds alone, Br prefers to bind to a surface oxygen. This happens because H acts as a Lewis base and forces Br to bind to a site on which it can function as a Lewis acid.[9,10]

The rules mentioned above are generalizations based on a limited number of calculations, and new examples will increase our confidence in their validity. Here we examine to what extent these rules are applicable when we adsorb a H atom or two H atoms on a $La_2O_3(001)$ surface. We study La_2O_3 because it is a model for other irreducible oxides (MgO, CaO, Sm_2O_3, etc.). These are often used as catalysts for partial oxidation of organic compounds, when a high reaction temperature is needed (e.g., oxidative methane coupling to produce ethane or ethylene, which is performed at 700 °C < T < 800 °C). Reducible oxides cannot be used at such high temperatures because they would combust the alkane.

Several results presented in this paper are briefly highlighted here.

(1) When one H atom is adsorbed on La_2O_3, it will only bind to an oxygen atom to form a hydroxyl: all our attempts to induce H to bind to a La cation have failed.

(2) H adsorption on La_2O_3, to form a hydroxyl, is accompanied by the formation of a polaron in which the electron donated by H is shared by several (sometimes up to six) La ions. The polaron can be located on different sites on the surface (not necessarily near the hydroxyl) or below the surface. The energy of H adsorption is lowered by the formation of the polaron and depends on the location of the polaron with respect to the hydroxyl. The formation of a polaron on La_2O_3 is surprising. Electron donors (such as H)

Received: June 3, 2015
Revised: July 27, 2015
Published: August 13, 2015

DOI: 10.1021/acs.jpcc.5b05310
J. Phys. Chem. C 2015, 119, 19876−19882

form polarons easily when adsorbed on reducible oxides (e.g., TiO_2, CeO_2, V_2O_5) because the donated electron reduces a cation to a lower formal charge (e.g., Ti^{4+} and Ce^{4+} are converted to Ti^{3+} and Ce^{3+}).[13−22] This mechanism of polaron formation cannot work on stoichiometric, defectless, irreducible oxides because their cations will not lower their formal charge (e.g., La in La_2O_3 will not become La^{2+}). We were surprised to find that the electron donated by a H atom, bound to a surface oxygen to make a hydroxyl, forms a polaron by becoming localized between several La atoms. We have tried to make a similar polaron upon H adsorption on other irreducible oxides (MgO and CaO) but were unsuccessful. We note, however, that polarons are formed[23−26] on stepped surfaces of MgO, which is a typical irreducible oxide.

(3) The presence of a hydroxyl on the La_2O_3 surface causes a second H to bind to the group of La atoms that formed a polaron when the first hydroxyl was created. The H atom in the hydroxyl is positively charged, and the H atom bonded to the La group is negatively charged. Therefore, the hydrogen atom in the hydroxyl is a Lewis base, and its presence on the surface forces the second hydrogen to bind to the La group because in doing so it becomes a Lewis acid. We emphasize that, in the absence of the first hydroxyl, H does not bind to La cations. An equivalent way of stating these results is to say that the polaron formed by the group of La ions is a basic Lewis site and H, being amphoteric, binds to it and becomes a Lewis acid. A similar situation has been seen for CH_4 dissociative adsorption on La_2O_3.[12] Both fragments (H and CH_3) formed by dissociative adsorption prefer to bind to a surface oxygen atom if alone on the surface. However, when bonded together, one binds to oxygen and the other to La because in this configuration one acts as a Lewis acid and the other as a Lewis base. The formation of this Lewis acid−Lewis base pair stabilizes the fragments. We propose that this is a general feature when two amphoteric compounds bind to an irreducible oxide.

2. COMPUTATIONAL DETAILS

We used the Vienna Ab Initio Package (VASP)[27−30] to perform spin-polarized density functional calculations, with the Perdew−Burke−Ernzerhof (PBE) exchange and correlation functional.[31] Scalar relativistic projected augmented wave (PAW)[32,33] pseudopotentials describe the ionic cores. Eleven valence electrons, six valence electrons, and 1 valence electron were explicitly taken into account for La, O, and H, respectively, using a plane wave basis set with an energy cutoff of 400 eV. The effect of spin−orbit coupling was ignored.

The number of unpaired electrons (N_s) was kept constant during geometry optimization. N_s is the difference between the number of occupied spin-up and spin-down orbitals. Calculations were performed for various values of N_s. We report only the results for the N_s values that give the lowest energy.

The Harris−Foulkes correction was applied when we calculated forces. The Kohn−Sham matrix was diagonalized iteratively using the Davidson block iteration. Fractional occupancies of the bands were allowed using the Gaussian smearing method with a window of 0.05 eV.

The La_2O_3(001) surface was modeled using a hexagonal [4 × 4] supercell and a slab composed of three stoichiometric (15 atomic) layers. The structure shown in Figure 1a is a stoichiometric layer viewed from the side. L1, L3, and L5 label successive oxygen atom layers, and L2 and L4 the La layers. The structure shown in Figure 1b is a top view of the [4 × 4] supercell. Note that Figure 1 shows a slab on which a H atom is adsorbed to make a hydroxyl (the cyan sphere is the oxygen in the hydroxyl, and the small blue sphere is a hydrogen atom in the hydroxyl).

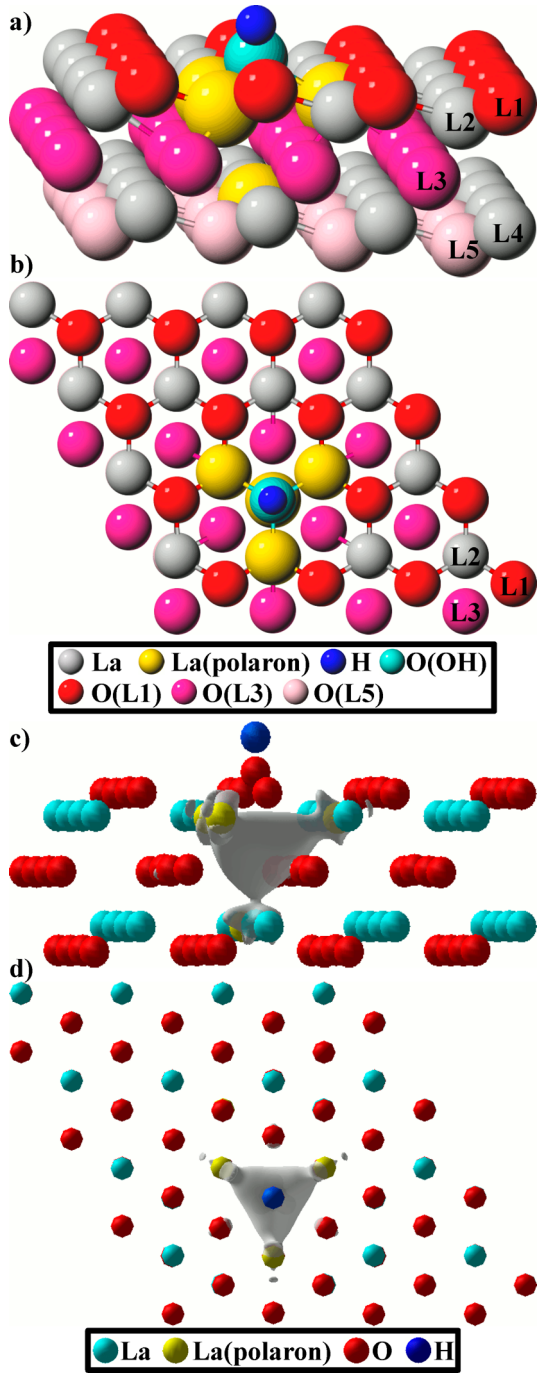

Figure 1. Structure of the lowest energy state for a H atom adsorbed on an oxygen atom on the clean stoichiometric La_2O_3(001) surface. (a) Side view showing one stoichiometric (five atomic) layer. (b) Same structure viewed from the top. The hydrogen atom is blue, the oxygen atom to which H is bonded is cyan, and the four La atoms that form the polaron are yellow. The labels L1 to L5 indicate the positions of the layers with respect to the vacuum space. (c, d) Side and top views of the equal-density surface (0.015 e/Å^3) of the spin-up highest occupied molecular orbital.

A vacuum space of 15 Å was inserted between the slab and its periodic replicas along the direction perpendicular to the (001)

DOI: 10.1021/acs.jpcc.5b05310
J. Phys. Chem. C 2015, 119, 19876−19882

surface. During geometry optimization, the atoms in the bottom stoichiometric layer were held fixed at their bulk positions. The positions of the remaining atoms were varied until the *x*-, *y*-, and *z*-components of the first derivatives of the energy with respect to the nuclear positions were smaller than 0.01 eV/Å. The geometry optimization was performed using the limited-memory Broyden−Fletcher−Goldfarb−Shanno algorithm implemented in the VASP Transition State Tool package (this toolkit can be downloaded from http://theory.cm.utexas.edu/vtsttools/). The convergence criterion was 10^{-5} eV for the self-consistent electronic minimization. No symmetry was imposed during geometry optimization.

Monopole, dipole, and quadrupole corrections to the energy were applied in the direction perpendicular to the slab to cancel the electrostatic interaction between the slab and its periodic images.[34] Due to the size of the supercell, the Brillouin zone was sampled at the Γ-point only. The relative energies are converged within 0.1 eV on the basis of tests performed using an automatically generated Γ-centered 2 × 2 × 1 Monkhorst−Pack[35] grid and a smaller [3 × 3] supercell.

Vibrational frequencies were obtained using the harmonic approximation. The second derivatives of the energy with respect to the nuclear positions (Hessian) were obtained by finite differences of the analytical gradients using a step size of 0.015 Å. Most of the atoms of the surface were held fixed to reduce the computational effort associated with the evaluation of the numerical Hessian matrix. The only atoms allowed to move were the two hydrogen atoms, the oxygen atom of the hydroxyl, the La atoms bonded to the hydride, and the oxygen atoms contributing to the highest occupied molecular orbital (HOMO). These oxygen atoms were identified from the density plot of the HOMO (see the right column in Figure S2).

The atomic volumes used in the Bader charge analysis[36−39] were determined using the total (core + valence) electronic density. The atomic spin polarization (for which we use the symbol n_s) is obtained by determining how much of the total spin density of the valence electrons is located within the Bader atomic volume of one atom, or a group of atoms. It is calculated using

$$n_s[\mathrm{M}] = \int_{V_B[\mathrm{M}]} \mathrm{d}\vec{r}\ |\rho_\uparrow(\vec{r}) - \rho_\downarrow(\vec{r})| \tag{1}$$

Here, M is an atom or a group of atoms, $V_B[\mathrm{M}]$ is the Bader volume of M, $\rho_\uparrow(\vec{r})$ is the density of the spin-up valence electrons, and $\rho_\uparrow(\vec{r})$ is the density of the spin-down valence electrons.

The density $\rho_M[i]$ of a spin−orbital φ_i located within the volume of an atom or a group of atoms is obtained from

$$\rho_M[i] = \int_{V_B[\mathrm{M}]} \mathrm{d}\vec{r}\ \varphi_i(\vec{r})^*\, \varphi_i(\vec{r}) \tag{2}$$

It is widely accepted that a hybrid functional gives more reliable results than GGA. For this reason, we have performed some calculations with the Heyd, Scuseria, and Ernzerof 2006 functional (HSE06)[40−43] to validate our qualitative findings regarding the adsorption of two hydrogen atoms. To reduce the computational cost associated with HSE06, we have studied a limited number of structures, performed spin-nonpolarized calculations, and used a [3 × 3] supercell and a slab composed of two stoichiometric (10 atomic) layers.

3. ADSORPTION OF ONE HYDROGEN ATOM

A hydrogen atom adsorbed on $La_2O_3(001)$ will bind only on a surface oxygen. All our attempts to induce H to bind to a La ion or a group of La ions failed: all geometry optimizations that started with H near La ended with H adsorbed on a surface oxygen. The energy of the reaction $^1/_2H_2 + La_2O_3 \rightleftarrows H{-}O/La_2O_3$ is +1.48 eV; the positive sign means that the reaction is endoergic. The notation $H{-}O/La_2O_3$ indicates that a H atom is bonded to a surface oxygen to make a hydroxyl. This hydrogen is an electron donor, and it injects, so to speak, an electron into the oxide. Since La_2O_3 is irreducible, this electron is not localized on one ion to convert it to a lower formal charge La^{2+} (as would happen if the oxide were reducible). However, the electron can make different polarons by being localized on different groups of La atoms. These polarons differ through their location and through the number of La atoms involved in them. Figure 1 shows the structure of the lowest energy $H{-}O/La_2O_3$ surface on which a polaron was formed following the adsorption of one H atom. The hydrogen atom is blue, the oxygen that is part of the hydroxyl is cyan, and the four La atoms involved in the polaron are yellow. The most stable OH−polaron system has the polaron under the hydroxyl.

There are several reasons why we know that a polaron is formed: (1) The La ions where the polaron is located are displaced from the position they had before H adsorption. (2) The formation of a hydroxyl changes the charge on the four La atoms forming the polaron by −0.38 electron (see Table S1). (3) The spin density on the four La atoms involved in the polaron changes from zero (prior to H adsorption) to 0.56 electron (after H adsorption). (4) The shape of the spin-up HOMO is a triangular pyramid with the corners of the triangle located on three La atoms in the first layer and the tip located on a La atom in the second La layer (see Figure 1c,d). The total HOMO electron density in the Bader volume of the four La atoms is 0.61 electron. The largest electron density is in the space between the four La atoms that form the polaron.

The polaron giving the lowest energy forms spontaneously during geometry optimization. Those having higher energy (hence being metastable) are created by one of the following two methods. In the first method, we optimize the geometry in two stages: We fix the La atoms in positions that seem appropriate for a polaron, mostly consisting in moving the La atoms closer to each other and displacing away the oxygen atom located closest to the center of the polaron. Then we optimize the structure without allowing the positions of the La atoms to change. After the structure is optimized, we release the hold on the La atoms and allow all atoms to move to positions that minimize the total energy. In most cases, the electron remains trapped at the distorted site, and the final state obtained in this way is a local minimum on the potential energy surface. The second method, which works just as well, is to adsorb two hydrogen atoms, one forming a hydroxyl and the other one placed between the La atoms where we want the polaron to be formed. We optimize the geometry, then remove the H atom bound to the group of La atoms, and optimize the structure again. In almost all cases, the system will make a polaron at the site where the removed H was located. We will explain why this method works in the next section.

As we have already mentioned, the polaron can be made at a variety of locations with respect to the hydroxyl. Five such locations which are representative of all possibilities are shown in Figure S1. Table S1 gives the formation energies of these five

DOI: 10.1021/acs.jpcc.5b05310
J. Phys. Chem. C 2015, 119, 19876−19882

polarons, their Bader charges, their spin densities, the energies of their HOMOs, and the electron density of the HOMO located in the Bader volume of each polaron. Placing the polaron in different locations changes the energy of hydroxyl formation by at most 0.25 eV. This means that at the temperatures used in catalysis all these locations have a fair probability of being present in the system. We also expect the polaron to be mobile but did not attempt to calculate the activation energy to move it from site to site.

We have tried unsuccessfully to make polarons when H is adsorbed on MgO and CaO, which are also irreducible oxides. It is not clear what causes the difference between these two oxides and La_2O_3.

In the next section, we show that a second hydrogen atom bonding to the surface will adsorb at a polaron site (created by the preadsorbed H) to form a hydride. The polaron is a strong Lewis base site which forces the second H atom to behave as a Lewis acid, in spite of the fact that when H is adsorbed alone, it is a Lewis base.

4. COADSORPTION OF TWO HYDROGEN ATOMS

4.1. Introduction. Since one hydrogen atom binds to an oxygen atom, and refuses to make a bond at a La site, one might suspect that a second H atom will also bind to a surface oxygen. If this were the case, the coadsorption would not benefit from the stabilization that takes place when one adsorbate is a Lewis acid and the other is a Lewis base.[8] An alternative is that one H atom binds to the oxygen, and acts as a Lewis base, and the other binds somewhere in the vicinity of a La atom or a group of La atoms to become a Lewis acid. This would create an acid−base pair, and this will substantially lower the adsorption energy. We can think of the adsorption of two H atoms as taking place successively. The first atom adsorbs to make a hydroxyl and a polaron. Then the second atom can become a Lewis acid by taking the electron from the polaron and becoming a hydride (H^-) with a formal charge of −1. According to the Lewis acid−base rules, the hydroxyl−hydride configuration should have a substantially lower energy than the hydroxide−hydroxide configuration. In what follows, we present calculations that show that this prediction of the acid−base rules is correct.

4.2. Formation of Two Hydroxyls. The adsorption of two H atoms to form two hydroxyls is possible, and it is endoergic by 2.92 eV (this is the energy of the reaction $H_2 + La_2O_3 \rightleftarrows H{-}O/H{-}O/La_2O_3$, where $H{-}O/H{-}O/La_2O_3$ indicates that two hydroxyls are present on the surface in the final state). The energy to adsorb one hydroxyl (the energy of the reaction $^1/_2H_2 + La_2O_3 \rightleftarrows H{-}O/La_2O_3$) is 1.48 eV. The energy of making two hydroxyls is close to twice the energy to form one hydroxyl. There is essentially no interaction between hydroxyls, and the reaction energy is independent of the distance between the hydroxyls. The creation of a second hydroxyl injects a second electron into the oxide. We found that the two electrons prefer to have opposite spins and to be located on the hydroxyls (see Table S2).

4.3. Formation of a Hydroxyl and a Hydride. On the basis of the rules we have already discussed, we expect that the energy of the dissociative adsorption of H_2 is lower if one of the hydrogens forms a hydroxyl and the other forms a hydride (by binding at the location of the polaron formed when the first hydroxyl is created). Since the polaron formed by the hydroxyl can be located at different sites relative to the hydroxyl, so can the hydride (see Figure S2). In Figure 2, we show the lowest energy structure for a hydroxyl−hydride pair. We colored cyan the surface oxygen to which one H atom is bound to form a hydroxyl. The yellow spheres show the four La atoms involved in polaron formation. They form a triangular pyramid with the base in the surface La layer (L2) and the tip in the second La layer (L4). The hydroxyl is located in the center of the

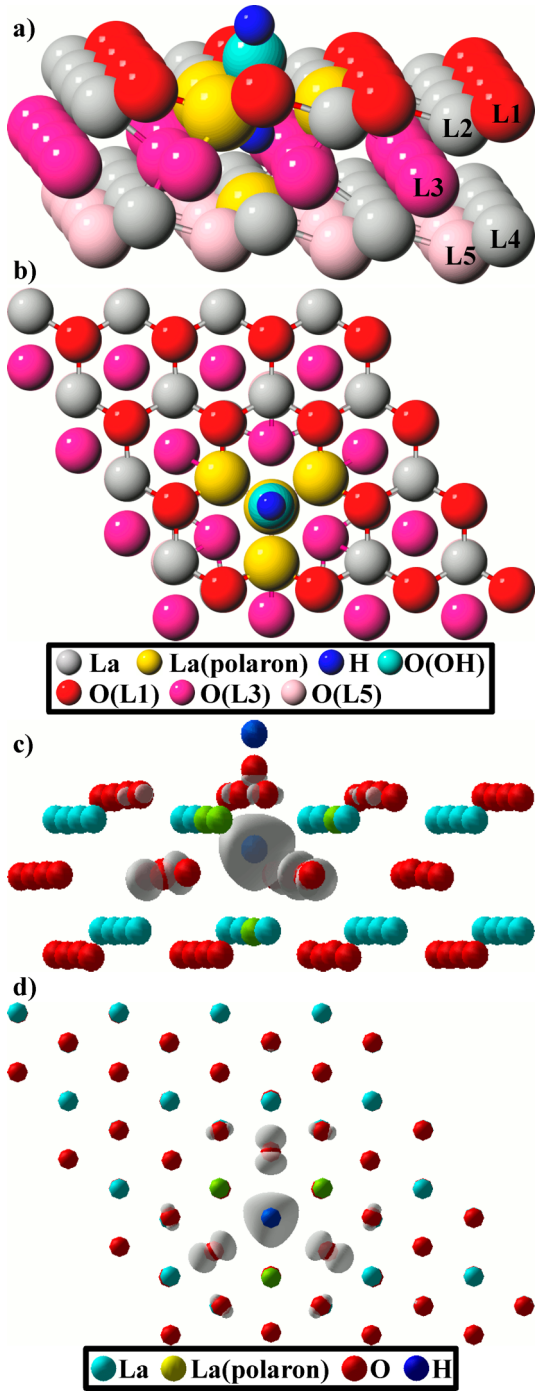

Figure 2. (a, b) Side and top views of the lowest energy structure for the formation of a hydroxyl−hydride pair when two H atoms are coadsorbed. The oxygen atom that is part of the hydroxyl is cyan, and the hydrogen atoms are blue. The group of four La atoms that form a polaron are yellow; they form a triangular pyramid with the hydride H atom roughly in the center. For hydride configurations having higher energy, see Figure S2. (c, d) Side and top views of the equal-density surface (0.015 e/Å^3) of the spin-up highest occupied molecular orbital.

DOI: 10.1021/acs.jpcc.5b05310
J. Phys. Chem. C 2015, 119, 19876−19882

polaron's triangular base, and the hydride is located in the center of the La pyramid. Essentially, the hydride is located where the probability of finding the electron of the polaron is high. Row 5 of Table S3 gives information about the hydroxyl−hydride structure having the lowest energy. The energy of the reaction $H_2 + La_2O_3 \rightleftarrows (H{-}O,H{-}La)/La_2O_3$ is 0.64 eV. The reaction is endoergic, but hydroxyl−hydride formation is substantially more favorable than the hydroxide−hydroxide formation (whose energy is 2.92 eV). The acid−base interaction lowers the dissociative adsorption energy by 2.92 eV − 0.64 eV = 2.28 eV.

Our statement that one hydrogen forms a hydride is supported by the results given in row 5 of Table S3. The Bader charge on the hydride hydrogen is −0.59 electron, meaning that the atom has an electron excess compared to the neutral hydrogen atom. The shape of the HOMO confirms the formation of a hydride. The density plot of the HOMO (see Figures 2c,d) shows a large lobe surrounding the hydride and a smaller contribution from the closest oxygen atoms of the surface. The interaction between the negatively charged hydrogen and nearby oxygen atoms is antibonding. The repulsive interaction forces the oxygen atoms located closest to the hydride to move away from their lattice position. The displacements are significant. We have observed a position shift of over 1 Å.

The harmonic vibrational frequencies given in Table S4 show that the frequency associated with the vibration of the hydride is very different from the frequency associated with the stretching of the O−H bond. Thus, vibrational frequencies can be used to experimentally differentiate the hydroxyl from the hydride.

5. DISCUSSION

The calculations presented here show that the adsorption of one H atom on lanthana takes place on a surface oxygen atom to form a hydroxyl and a polaron. The formation of a polaron on an irreducible oxide is surprising. It is possible because the electron donated when the hydroxyl is formed is delocalized over several La atoms. This is different from reducible oxides where hydroxyl formation takes place with the reduction of one cation of the host oxide. The energy of hydroxyl formation depends on the location of the polaron; in the lowest energy structure, the polaron is under the hydroxyl. When two hydrogen atoms are adsorbed, one forms a hydroxyl and the other a hydride with the negative H atom located in the center of the La triangular pyramid where the polaron was located. This behavior is consistent with the rule that if two amphoteric compounds are coadsorbed, they will prefer binding sites on which one adsorbate is a Lewis acid and the other a Lewis base.

It appears that the formation of a polaron upon adsorption of one H atom is a feature specific to lanthana: our attempts to create a polaron on MgO or CaO failed. We propose however that the tendency of adsorbates to bind so that they form an acid−base pair is general. Another way of saying this is to state that the dissociation of H_2 on the surface of an irreducible oxide is heterolytic. Since the vibrational frequency of the hydroxyl is very different from that of the hydride, the detection of the two species by infrared spectroscopy is possible. Experiments have detected both hydroxyls and hydrides on gallium oxide,[44−46] magnesium oxide,[47,48] ruthenium oxide,[49] zinc oxide,[50−54] zirconium oxide,[55−57] and aluminum oxide.[58] The situation on reducible oxides is not as clear because the electron donated by the hydroxyl can be used to either reduce a cation in the host oxide (e.g., convert Ti^{4+} to Ti^{3+}) or form a hydride with a second H atom. In other words, the hydride competes with the cations for the electron donated by the hydroxyl. It appears that the formation of the acid−base pair by the adsorbed species prevails.[10,59,60]

To test the reliability of the qualitative conclusions obtained by using the PBE functional, we performed a number of calculations using the HSE06 functional. The results are given in the Table S5 and Table S6. For a given structure, the difference between the H_2 dissociative adsorption energy obtained using the two functionals varies by at most 0.25 eV. The energy of the HOMO varies by as much as 0.5 eV, but the shapes of the orbitals obtained using both functionals are very similar. Because we are interested in general trends and the results obtained using the PBE and HSE06 functionals are in qualitative agreement, we are confident that the qualitative statements based on calculations with the PBE functional (without a U correction) are reliable. This is consistent with previous work showing that the inclusion of the on-site Coulomb repulsion (U) is not needed for the description of a $La_2O_3(001)$ surface having a missing oxygen atom.[61]

■ ASSOCIATED CONTENT

Supporting Information

The Supporting Information is available free of charge on the ACS Publications website at DOI: 10.1021/acs.jpcc.5b05310.

Figures showing the low-energy structures formed by bonding a neutral hydrogen atom to a surface oxygen atom and by the coadsorption of two hydrogen atoms, tables of the properties of the polarons, hydroxyl, and hydride, and comparison of PBE and HSE06 functionals (PDF)

■ AUTHOR INFORMATION

Corresponding Author

*Phone: 805-893-2256. Fax: 805-893-4120. E-mail: metiu@chem.ucsb.edu.

Notes

The authors declare no competing financial interest.

■ ACKNOWLEDGMENTS

Financial support was provided by the Air Force Office of Scientific Research (Grant FA9550-12-1-0147) and the Department of Energy, Office of Science, Office of Basic Energy Sciences (Grant DE-FG03-89ER14048). We acknowledge support from the Center for Scientific Computing at the California NanoSystems Institute and the UCSB (University of California, Santa Barbara) Materials Research Laboratory (a National Science Foundation Materials Research Science and Engineering Center (NSF MRSEC), Grant DMR-1121053) funded in part by NSF Grant CNS-0960316 and Hewlett-Packard. Use of the Center for Nanoscale Materials was supported by the U.S. Department of Energy, Office of Science, Office of Basic Energy Sciences, under Contract DE-AC02-06CH11357.

■ REFERENCES

(1) Schneider, W. F.; Hass, K. C.; Miletic, M.; Gland, J. L. Dramatic cooperative effects in adsorption of NO_x on MgO(001). *J. Phys. Chem. B* **2002**, *106*, 7405−7413.

DOI: 10.1021/acs.jpcc.5b05310
J. Phys. Chem. C 2015, 119, 19876−19882

(2) Broqvist, P.; Panas, I.; Fridell, E.; Persson, H. NO_x storage on BaO(100) surface from first principles: A two channel scenario. *J. Phys. Chem. B* **2002**, *106*, 137−145.
(3) Broqvist, P.; Grönbeck, H.; Fridell, E.; Panas, I. Characterization of NO_x Species adsorbed on BaO: Experiment and theory. *J. Phys. Chem. B* **2004**, *108*, 3523−3530.
(4) Schneider, W. F. Qualitative differences in the adsorption chemistry of acidic (CO_2, SO_x) and amphiphilic (NO_x) species on the alkaline earth oxides. *J. Phys. Chem. B* **2004**, *108*, 273−282.
(5) Grönbeck, H.; Broqvist, P.; Panas, I. Fundamental aspects of NO_x adsorption on BaO. *Surf. Sci.* **2006**, *600*, 403−408.
(6) Chrétien, S.; Metiu, H. Enhanced adsorption energy of Au_1 and O_2 on the stoichiometric TiO_2(110) surface by coadsorption with other molecules. *J. Chem. Phys.* **2008**, *128*, 044714.
(7) Mei, D.; Ge, Q.; Szanyi, J.; Peden, H. F. First-principles analysis of NO_x adsorption on anhydrous γ-Al_2O_3 surfaces. *J. Phys. Chem. C* **2009**, *113*, 7779−7789.
(8) Metiu, H.; Chrétien, S.; Hu, Z.; Li, B.; Sun, X. Chemistry of Lewis acid-base pairs on oxide surfaces. *J. Phys. Chem. C* **2012**, *116*, 10439−10450.
(9) Li, B.; Metiu, H. Does halogen adsorption activate the oxygen atom on an oxide surface? I. A study of Br_2 and HBr adsorption on La_2O_3 and La_2O_3 doped with Mg or Zr. *J. Phys. Chem. C* **2012**, *116*, 4137−4148.
(10) Hu, Z.; Metiu, H. Halogen adsorption on CeO_2: The role of Lewis acid-base pairing. *J. Phys. Chem. C* **2012**, *116*, 6664−6671.
(11) McFarland, E. W.; Metiu, H. Catalysis by doped oxides. *Chem. Rev.* **2013**, *113*, 4391−4427.
(12) Chrétien, S.; Metiu, H. Acid−base interaction and its role in alkane dissociative chemisorption on oxide surfaces. *J. Phys. Chem. C* **2014**, *118*, 27336−27342.
(13) Shibuya, T.; Yasuoka, K.; Mirbt, S.; Sanyal, B. Bipolaron formation induced by oxygen vacancy at rutile TiO_2(110) Surfaces. *J. Phys. Chem. C* **2014**, *118*, 9429−9435.
(14) Di Valentin, C.; Pacchioni, G.; Selloni, A. Reduced and n-type doped TiO_2: Nature of Ti^{3+} species. *J. Phys. Chem. C* **2009**, *113*, 20543−20552.
(15) Chrétien, S.; Metiu, H. Electronic structure of partially reduced rutile TiO_2(110) surface: Where are the unpaired electrons located? *J. Phys. Chem. C* **2011**, *115*, 4696−4705.
(16) Deskins, N. A.; Rousseau, R.; Dupuis, M. Localized electronic states from surface hydroxyls and polarons in TiO_2(110). *J. Phys. Chem. C* **2009**, *113*, 14583−14586.
(17) Deskins, N. A.; Rousseau, R.; Dupuis, M. Defining the role of excess electrons in the surface chemistry of TiO_2. *J. Phys. Chem. C* **2010**, *114*, 5891−5897.
(18) Deskins, N. A.; Rousseau, R.; Dupuis, M. Distribution of Ti^{3+} surface sites in reduced TiO_2. *J. Phys. Chem. C* **2011**, *115*, 7562−7572.
(19) Ganduglia-Pirovano, M. V.; Da Silva, J. L. F.; Sauer, J. Density-Functional calculations of the structure of near-surface oxygen vacancies and electron localization on CeO_2(111). *Phys. Rev. Lett.* **2009**, *102*, 026101.
(20) Paier, J.; Penschke, C.; Sauer, J. Oxygen defects and surface chemistry of ceria: Quantum chemical studies compared to experiment. *Chem. Rev.* **2013**, *113*, 3949−3985.
(21) Li, H. Y.; Wang, H. F.; Gong, X. Q.; Guo, Y. L.; Guo, Y.; Lu, G. Z.; Hu, P. Multiple configurations of the two excess 4f electrons on defective CeO_2(111): Origin and implications. *Phys. Rev. B: Condens. Matter Mater. Phys.* **2009**, *79*, 193401.
(22) Kristoffersen, H. H.; Metiu, H. Reconstruction of low-index α-V_2O_5 surfaces. *J. Phys. Chem. C* **2015**, *119*, 10500−10506.
(23) Pacchioni, G.; Freund, H. Electron transfer at oxide surfaces. The MgO paradigm: From defects to ultrathin films. *Chem. Rev.* **2013**, *113*, 4035−4072.
(24) Chiesa, M.; Paganini, M. C.; Giamello, E.; Murphy, D. M.; Di Valentin, C.; Pacchioni, G. Excess electrons stabilized on ionic oxide surfaces. *Acc. Chem. Res.* **2006**, *39*, 861−867.
(25) Ricci, D.; Di Valentin, C.; Pacchioni, G.; Sushko, P. V.; Shluger, A. L.; Giamello, E. Paramagnetic defect centers at the MgO surface. An alternative model to oxygen vacancies. *J. Am. Chem. Soc.* **2003**, *125*, 738−747.
(26) Chiesa, M.; Paganini, M. C.; Giamello, E.; Di Valentin, C.; Pacchioni, G. Electron traps on oxide surfaces: (H+)(e−) pairs stabilized on the surface of ^{17}O enriched CaO. *ChemPhysChem* **2006**, *7*, 728−734.
(27) Kresse, G.; Hafner, J. Ab-initio molecular-dynamics for liquid-metals. *Phys. Rev. B: Condens. Matter Mater. Phys.* **1993**, *47*, 558−561.
(28) Kresse, G.; Hafner, J. Ab-Initio molecular-dynamics simulation of the liquid-metal amorphous-semiconductor transition in germanium. *Phys. Rev. B: Condens. Matter Mater. Phys.* **1994**, *49*, 14251−14269.
(29) Kresse, G.; Furthmuller, J. Efficient iterative schemes for ab initio total-energy calculations using a plane-wave basis set. *Phys. Rev. B: Condens. Matter Mater. Phys.* **1996**, *54*, 11169−11186.
(30) Kresse, G.; Furthmüller, J. Efficiency of ab-initio total energy calculations for metals and semiconductors using a plane-wave basis set. *Comput. Mater. Sci.* **1996**, *6*, 15−50.
(31) Perdew, J. P.; Burke, K.; Ernzerhof, M. Generalized gradient approximation made simple. *Phys. Rev. Lett.* **1996**, *77*, 3865−3868.
(32) Blöchl, P. E. Projector augmented-wave method. *Phys. Rev. B: Condens. Matter Mater. Phys.* **1994**, *50*, 17953−17979.
(33) Kresse, G.; Joubert, D. From ultrasoft pseudopotentials to the projector augmented-wave method. *Phys. Rev. B: Condens. Matter Mater. Phys.* **1999**, *59*, 1758−1775.
(34) Makov, G.; Payne, M. C. Periodic boundary-conditions In ab-initio calculations. *Phys. Rev. B: Condens. Matter Mater. Phys.* **1995**, *51*, 4014−4022.
(35) Monkhorst, H. J.; Pack, J. D. Special points for Brillouin-zone integrations. *Phys. Rev. B* **1976**, *13*, 5188−5192.
(36) Bader, R. *Atoms in Molecules: A Quantum Theory*; Clarendon: Oxford, U.K., 1994.
(37) Tang, W.; Sanville, E.; Henkelman, G. A grid-based Bader analysis algorithm without lattice bias. *J. Phys.: Condens. Matter* **2009**, *21*, 084204.
(38) Sanville, E.; Kenny, S. D.; Smith, R.; Henkelman, G. Improved grid-based algorithm for Bader charge allocation. *J. Comput. Chem.* **2007**, *28*, 899−908.
(39) Henkelman, G.; Arnaldsson, A.; Jonsson, H. A fast and robust algorithm for Bader decomposition of charge density. *Comput. Mater. Sci.* **2006**, *36*, 354−360.
(40) Heyd, J.; Peralta, J. E.; Scuseria, G. E.; Martin, R. L. Energy band gaps and lattice parameters evaluated with the Heyd-Scuseria-Ernzerhof screened hybrid functional. *J. Chem. Phys.* **2005**, *123*, 174101.
(41) Heyd, J.; Scuseria, G. Efficient hybrid density functional calculations in solids: Assessment of the Heyd-Scuseria-Ernzerhof screened Coulomb hybrid functional. *J. Chem. Phys.* **2004**, *121*, 1187−1192.
(42) Heyd, J.; Scuseria, G. E. Assessment and validation of a screened Coulomb hybrid density functional. *J. Chem. Phys.* **2004**, *120*, 7274−7280.
(43) Heyd, J.; Scuseria, G. E.; Ernzerhof, M. Hybrid functionals based on a screened Coulomb potential. *J. Chem. Phys.* **2003**, *118*, 8207−8215.
(44) Pan, Y.-x.; Mei, D.; Liu, C.-j.; Ge, Q. Hydrogen adsorption on Ga_2O_3 surface: A combined experimental and computational study. *J. Phys. Chem. C* **2011**, *115*, 10140−10146.
(45) Meriaudeau, P.; Primet, M. FTIR study of hydrogen adsorption on α-Ga_2O_3. *J. Mol. Catal.* **1990**, *61*, 227−234.
(46) Collins, S. E.; Baltanás, M. A.; Bonivardi, A. L. Hydrogen chemisorption on gallium oxide polymorphs. *Langmuir* **2005**, *21*, 962−970.
(47) Gribov, E. N.; Bertarione, S.; Scarano, D.; Lamberti, C.; Spoto, G.; Zecchina, A. Vibrational and thermodynamic properties of H_2 adsorbed on MgO in the 300−20 K interval. *J. Phys. Chem. B* **2004**, *108*, 16174−16186.

DOI: 10.1021/acs.jpcc.5b05310
J. Phys. Chem. C 2015, 119, 19876−19882

(48) Diwald, O.; Hofmann, P.; Knozinger, E. H_2 chemisorption and consecutive UV stimulated surface reactions on nanostructured MgO. *Phys. Chem. Chem. Phys.* **1999**, *1*, 713−721.
(49) Wei, Y.; Martinez, U.; Lammich, L.; Besenbacher, F.; Wendt, S. Formation of metastable, heterolytic H-pairs on the RuO_2(110) surface. *Surf. Sci.* **2014**, *619*, L1−L5.
(50) Boccuzzi, F.; Borello, E.; Zecchina, A.; Bossi, A.; Camia, M. Infrared study of ZnO surface properties: I. Hydrogen and deuterium chemisorption at room temperature. *J. Catal.* **1978**, *51*, 150−159.
(51) Griffin, G. L.; Yates, J. T., Jr. Combined temperature-programmed desorption and infrared study of H_2 chemisorption on ZnO. *J. Catal.* **1982**, *73*, 396−405.
(52) Griffin, G. L.; Yates, J. T., Jr. Adsorption studies of H_2 isotopes on ZnO: Coverage-induced IR frequency shifts and adsorbate geometry. *J. Chem. Phys.* **1982**, *77*, 3744−3750.
(53) Naito, S.; Shimizu, H.; Hagiwara, E.; Onishi, T.; Tamaru, K. Behaviour of chemisorbed hydrogen under reaction conditions and the mechanism of the H_2-D_2 exchange reaction over zinc oxide. *Trans. Faraday Soc.* **1971**, *67*, 1519−1528.
(54) Howard, J.; Braid, I. J.; Tomkinson, J. Spectroscopic studies of hydrogen adsorbed on zinc oxide (kadox 25). *J. Chem. Soc., Faraday Trans. 1* **1984**, *80*, 225−235.
(55) Onishi, T.; Abe, H.; Maruya, K.-i.; Domen, K. IR spectra of hydrogen adsorbed on ZrO_2. *J. Chem. Soc., Chem. Commun.* **1985**, 617−618.
(56) Kondo, J.; Sakata, Y.; Domen, K.; Maruya, K.-i.; Onishi, T. Infrared study of hydrogen adsorbed on ZrO_2. *J. Chem. Soc., Faraday Trans.* **1990**, *86*, 397−401.
(57) Kondo, J.; Domen, K.; Maruya, K.-i.; Onishi, T. Infrared study of molecularly adsorbed H_2 on ZrO_2. *Chem. Phys. Lett.* **1992**, *188*, 443−445.
(58) Joubert, J.; Salameh, A.; Krakoviack, V.; Delbecq, F.; Sautet, P.; Copéret, C.; Basset, J. M. Heterolytic splitting of H_2 and CH_4 on γ-alumina as a structural probe for defect sites. *J. Phys. Chem. B* **2006**, *110*, 23944−23950.
(59) García-Melchor, M.; López, N. Homolytic products from heterolytic paths in H_2 dissociation on metal oxides: The example of CeO_2. *J. Phys. Chem. C* **2014**, *118*, 10921−10926.
(60) Fernández-Torre, D.; Carrasco, J.; Ganduglia-Pirovano, M. V.; Pérez, R. Hydrogen activation, diffusion, and clustering on CeO_2(111): A DFT+U study. *J. Chem. Phys.* **2014**, *141*, 014703.
(61) Li, B.; Metiu, H. DFT studies of oxygen vacancies on undoped and doped La_2O_3 surfaces. *J. Phys. Chem. C* **2010**, *114*, 12234−12244.

DOI: 10.1021/acs.jpcc.5b05310
J. Phys. Chem. C 2015, 119, 19876−19882